JAM CM Journal of Applied Mathematics and Computational Mechanics 2026, 25(2), 67-82
www.amcm.pcz.pl p-ISSN 2299-9965
DOI: 10.17512/jamcm.2026.2.05 e-ISSN 2353-0588

ANALYSIS OF THE THERMOSTRESSED STATE OF A LEAD PLATE UNDER THE ACTION OF A QUASI-STATIC ELECTROMAGNETIC FIELD

Roman Musii[1], Myroslava Klapchuk[1], Viktor Pabyrivskyi[1]
Zenoviy Kohut[1,2], Dariusz Całus[2], Piotr Domanowski[3], Piotr Gębara[4]*

[1] *Institute of Applied Mathematics and Fundamental Sciences, Lviv Polytechnic National University*
Lviv, Ukraine
[2] *Faculty of Electrical Engineering, Czestochowa University of Technology*
Częstochowa, Poland
[3] *Faculty of Mechanical Engineering, Bydgoszcz University of Science and Technology*
Bydgoszcz, Poland
[4] *Faculty of Production Engineering and Materials Technology, Częstochowa University of Technology*
Częstochowa, Poland
roman.s.musii@lpnu.ua, myroslava.i.klapchuk@lpnu.ua, viktor.v.pabyrivskyi@lpnu.ua,
zenon.kogut@pcz.pl, dariusz.calus@pcz.pl, piotr.domanowski@pbs.edu.pl, piotr.gebara@pcz.pl

Received: 6 February 2026; Accepted: 4 May 2026

Abstract. A two-dimensional physical-mathematical model is proposed for analyzing the plane-deformed state of a nonferromagnetic plate under the action of a quasi-static electromagnetic field. Two-dimensional problems of electrodynamics, thermal conductivity, and thermoelasticity are formulated to find the determining functions, which are the tangential component of the magnetic field intensity vector, temperature, and components of the quasi-static stress tensor. To solve these problems, all determining functions are approximated by cubic polynomials in the thickness variable. This allows the initial two-dimensional problems for determining functions to be reduced to one-dimensional problems with respect to their integral characteristics. General solutions to problems for integral characteristics are obtained using a finite integral transform with respect to the transverse variable, as well as a Laplace integral transform with respect to the time variable. The change in time of the Fourier intensity of stresses in a lead plate under the action of a quasi-static electromagnetic field and their distribution across the plate cross-section at the moment of reaching maximum values are analyzed. The dependence of these quantities on the parameter characterizing surface and deep induction heating, as well as the conditions of convective heat transfer of the plate base and its side edges, is investigated.

MSC 2010: *74K25*
Keywords: *electroconductive plate, quasi-static electromagnetic field, near-surface and in-depth induction heating, stress intensities*

*Corresponding author

1. Introduction

Lead plates are widely used as shielding elements against external electromagnetic radiation and ionizing γ- and X-ray exposure in medical, scientific, and industrial facilities. In medical environments, such plates operate under electromagnetic fields generated by computed tomography scanners and other electrical diagnostic equipment [1].

Compared with other non-ferromagnetic metals, such as alloyed stainless steels and tungsten, lead exhibits a significantly lower melting temperature and elastic deformation limit. In addition, the application of lead in medical practice is associated with certain adverse effects on the human body [2]. These limitations have stimulated active research into structurally heterogeneous metal composite materials, in which lead is incorporated as a constituent phase in order to retain its favorable shielding properties while improving mechanical performance and reducing toxicity [3]. In particular, studies [4] support the incorporation of bismuth particles into nanocomposite systems, since bismuth possesses physical characteristics similar to those of lead and is recognized as a low-toxicity heavy metal.

Recent reviews [5, 6] are devoted to hybrid and newly developed materials for electromagnetic shielding. Traditionally, metals such as stainless steel, copper, aluminum, and silver have been preferred for shielding against electromagnetic interference due to their high shielding efficiency. However, the high electrical conductivity of metals often results in shielding through reflection, which can cause secondary electromagnetic pollution. Lead has viscous properties due to its internal structure, so its use as a protective shield minimizes secondary reflection.

The thermophysical behavior of metallic components subjected to electromagnetic excitation has also been investigated. For example, Lee et al. [7] analyzed the temperature distribution and bending response of a thick metal plate during high-frequency induction heating. Numerical simulation of induction heating processes involving coupled electromagnetic and thermal fields remains computationally demanding, particularly for ferromagnetic materials. To improve efficiency, Ref. [8] proposed a semi-analytical approach combining finite-element preprocessing with analytical electromagnetic formulations. Methods for analyzing the thermomechanical response of electroconductive elements are discussed in [9].

A number of studies [10, 11] examined the thermally stressed state of homogeneous and bimetallic plates using one-dimensional models under unsteady induction heating. In the study [12], a numerical framework combining electromagnetic, thermal, and mechanical processes was created to model the turbine rotor straightening process using induction heating. In the paper [13], a magneto-thermal bidirectional coupled model is developed to predict temperature fields under various structural factors. Numerical studies are conducted to optimize the structural parameters of the inductor to improve the welding strength of large-sized conductive plates. Temperature regimes and stress states have also been reported for plates made of copper [14] and tungsten [15].

Despite these achievements, the available literature contains insufficient analysis of the temperature change and stress-strain state of lead plates exposed to external quasi-static electromagnetic fields. Lead is a very soft and ductile material for which the elastic deformation zone is very short, which is shown in the diagram of the dependence of the stress intensity σ_i on the deformation intensity ε_i. The elastic deformation limit σ_d of pure lead and some alloys based on it is in the range 4-12 MPa.

Therefore, based on a validated two-dimensional physical-mathematical model, the present work aims to investigate the stress intensities arising in a lead plate under two induction heating regimes: near-surface and deep heating induced by a quasi-static electromagnetic field.

2. Thermomechanical problem formulation for an electroconductive plate

2.1. Problem description

In the Cartesian coordinate system $OX_1X_2X_3$ an electroconductive plate with thickness of $2h$ and a width of $2d_*$ is considered. Here h and d_* are dimensional half--thickness and half-width of the plate. The origin O is located at the symmetry center of the rectangular cross-section. The plate is assumed to be infinitely extended in the OX_2 direction, with its width aligned along OX_1 and its thickness along OX_3 (Fig. 1).

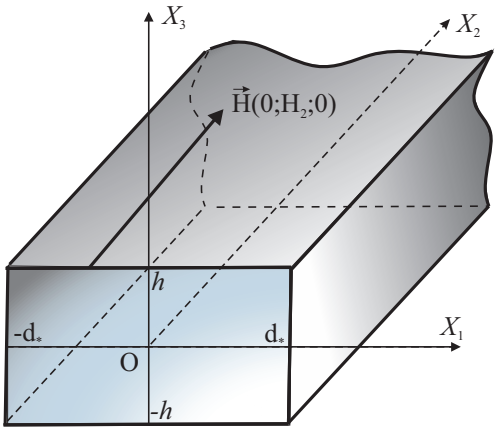

Fig. 1. An electroconductive plate of rectangular cross-section with thickness of $2h$ and a width of $2d_*$. The magnetic field inside the plate is described by the intensity vector $\vec{H} = \{0, H_2, 0\}$, where the component H_2 is directed parallel to the plate bases

The material of the plate is homogeneous, isotropic, and non-ferromagnetic. Its electrical, thermal, and mechanical characteristics are taken as constants corresponding to their averaged values over the heating process.

Induction heating is produced by an externally applied uniform quasi-static electromagnetic field. The induced currents give rise to Joule heat inside the plate, acting as time-dependent volumetric heat sources. These sources generate a transient temperature distribution, which subsequently leads to the development of thermally induced stresses.

To investigate this coupled process, a two-dimensional physical-mathematical framework is formulated and implemented in three successive steps. At the first stage, Maxwell's equations are employed to evaluate the electromagnetic field and the volumetric Joule heat generation. In the second stage, the heat conduction equation with internal heat sources is solved to obtain the temperature field. Finally, the thermostressed state of the plate is determined by solving the two-dimensional quasi-static thermoelasticity equations, yielding the components of the stress tensor. This sequential methodology enables a consistent description of the interaction between electromagnetic excitation, thermal response, and mechanical stresses in the conductive plate.

2.2. Definition of a two-dimensional electromagnetic field

The spatial coordinates x_1, x_2, x_3 are scaled by the half-thickness h, and the dimensionless variables $x_1 = X_1/h$, $x_2 = X_2/h$, and $x_3 = X_3/h$ are introduced. Accordingly, the normalized plate width is defined as $d = d_*/h$. Consider a magnetic field within a plate characterized by the intensity vector $\vec{H}(x_1, x_3, t) = \{0, H_2(x_1, x_3, t), 0\}$. The component $H_2(x_1, x_3, t)$ aligns with the bases of the plate at $x_3 = \pm 1$ and its end sections at $x_1 = \pm d$, while t represents time. This configuration enables the analysis of magnetic field diffusion in the plate.

To describe the spatial and temporal evolution of the component $H_2(x_1, x_3, t)$, we use the equation derived from Maxwell's relations [16]:

$$\left(\frac{\partial^2}{\partial x_1^2} + \frac{\partial^2}{\partial x_3^2} \right) H_2 - \frac{\partial H_2}{\partial \tau} = 0. \tag{1}$$

Here, the dimensionless time $\tau = \dfrac{t}{\sigma \mu h^2}$ governs the diffusion process, where σ and μ are the electrical conductivity and magnetic permeability of the plate material, respectively.

Boundary conditions for solving this equation are given by:

$$H_2\left(x_1,\, \pm 1,\, \tau\right) = H_2^{\pm(0)}\left(x_1,\, \tau\right), \tag{2}$$

$$H_2\left(\pm d,\, x_3,\, \tau\right) = H_2^{\pm(0)*}\left(x_3,\, \tau\right).$$

The functions $H_2^{\pm(0)}(x_1, \tau)$ and $H_2^{\pm(0)*}(x_3, \tau)$ define the magnetic field on the plate's surfaces.

If initially, at $\tau = 0$, the electromagnetic field (EMF) is absent, the initial condition is:

$$H_2(x_1,\, x_3,\, 0) = 0. \tag{3}$$

At the corners of the plate cross-section, continuity conditions for $H_2^{\pm(0)}$ and $H_2^{\pm(0)*}$ must be satisfied:

$$H_2^{+(0)}(d,\, \tau) = H_2^{+(0)*}(1,\, \tau), \quad H_2^{-(0)}(d,\, \tau) = H_2^{-(0)*}(-1,\, \tau),$$

$$H_2^{+(0)}(-d,\, \tau) = H_2^{-(0)*}(1,\, \tau), \quad H_2^{-(0)}(-d,\, \tau) = H_2^{-(0)*}(-1,\, \tau). \tag{4}$$

The associated electric field intensity vector $\vec{E}$ is determined as:

$$\vec{E} = \frac{1}{\sigma}\left(\mathrm{rot}\,\vec{H}\right). \tag{5}$$

The non-zero components of $\vec{E}$ are:

$$\vec{E}(x_1,\, x_3,\, \tau) = \{E_1(x_1,\, x_3,\, \tau);\, 0;\, E_3(x_1,\, x_3,\, \tau)\},$$

where:

$$E_1 = \frac{1}{\sigma}\frac{\partial H_2(x_1,\, x_3,\, \tau)}{\partial x_3}, \quad E_3 = \frac{1}{\sigma}\frac{\partial H_2(x_1,\, x_3,\, \tau)}{\partial x_1}.$$

The Joule heat density, given by $Q = \sigma\,\vec{E}^2$, can be expressed as:

$$Q = \frac{1}{\sigma}\left[\left(\frac{\partial H_2}{\partial x_1}\right)^2 + \left(\frac{\partial H_2}{\partial x_3}\right)^2\right]. \tag{6}$$

2.3. Definition of a two-dimensional temperature field

The temperature field $T(x_1,x_2,x_3,Fo)$ within the plate, influenced by time--dependent, continuously distributed Joule heat sources Q, can be evaluated using the heat conduction equation derived in [17]:

$$\left(\frac{\partial^2}{\partial x_1^2} + \frac{\partial^2}{\partial x_3^2}\right) T - \frac{\partial T}{\partial Fo} = -\frac{h^2}{\lambda} Q. \tag{7}$$

Here, $Fo = at/h^2$ represents the Fourier criterion, while a and λ denote the thermal diffusivity and thermal conductivity, respectively.

On the plate surfaces $x_3 = \pm 1$, the conditions for convective heat exchange with the external environment are given by:

$$\left(\frac{\partial T}{\partial x_3}\right)^{\pm} \pm Bi^{\pm}(T^{\pm} - T_c^{\pm}) = 0. \tag{8}$$

Here, $Bi^{\pm} = H^{\pm}h$ is the Biot criterion; $H^{\pm}$ is the relative heat transfer coefficient for the surfaces $x_3 = \pm 1$; $T^{\pm}$ and $\left(\frac{\partial T}{\partial x_3}\right)^{\pm}$ are the temperature and its gradient at the surfaces $x_3 = \pm 1$, respectively. $T_c^{\pm}$ represents the external environment temperatures at these surfaces, with initial values $T_c^{\pm}(x_1, x_2, 0) = T_c^{(0)}(x_1, x_2, 0)$, where $T_c^{(0)}$ denotes the initial external environment temperature.

Similarly, at the end sections of the plate $x_1 = \pm d$, convective heat exchange conditions are described as:

$$\left(\frac{\partial T}{\partial x_3}\right)^{*\pm} \pm Bi^{*\pm}(T^{*\pm} - T_c^{*\pm}) = 0. \tag{9}$$

The symbol $*$ in equation (9) indicates that these values are specific to the end sections $x_1 = \pm d$.

The initial temperature distribution within the plate at $Fo = 0$ is assumed to be:

$$T(x_1, x_2, x_3, 0) = T_c^{(0)}(x_1, x_2, 0). \tag{10}$$

2.4. Definition of a plane-deformed thermostressed state

It is known from previous studies [18] that during the induction heating of an electroconductive body by a quasi-static EMF, the stress state of this body is mainly determined by the Joule heat Q, and the influence of the ponderomotive forces $\vec{F}$ is negligible. Therefore, in the case of a plane deformation of a body with plane--parallel boundaries (plate) caused only by the temperature field $T(x_1, x_3, t)$. Thus, following [19] the governing system of equations of the two-dimensional quasi-static thermoelasticity problem has the form:

$$\left(\frac{\partial^2}{\partial x_1^2} + \frac{\partial^2}{\partial x_3^2}\right)\left(\psi^{(s)} + \frac{\alpha E T}{1-\nu}\right) = 0. \tag{11}$$

$$\left(\frac{\partial^2}{\partial x_1^2} + \frac{\partial^2}{\partial x_3^2}\right)\sigma_{13}^{(s)} = -\frac{\partial^2 \psi^{(s)}}{\partial x_1 \partial x_3}. \tag{12}$$

$$\frac{\partial^2 \sigma_{11}^{(s)}}{\partial x_1} = \frac{\partial^2 \sigma_{13}^{(s)}}{\partial x_3}. \tag{13}$$

$$\sigma_{33}^{(s)} = \psi^{(s)} - \sigma_{11}^{(s)}. \tag{14}$$

$$\sigma_{22}^{(s)} = \nu \psi^{(s)} - \alpha E T. \tag{15}$$

Here, $\sigma_{11}^{(s)}, \sigma_{22}^{(s)}, \sigma_{13}^{(s)}, \sigma_{33}^{(s)}$ are the components of the tensor $\hat{\sigma}^{(s)}$ of quasi-static stresses; $\psi^{(s)} = \sigma_{11}^{(s)} + \sigma_{33}^{(s)}$, α, ν are the linear thermal expansion and Poisson's ratios; E is the Young's modulus.

The boundary conditions on the surfaces $x_3 = \pm h$ of the plate are

$$\frac{\partial \psi^{(s)\pm}}{\partial x_1} + \frac{\partial \sigma_{13}^{(s)\pm}}{\partial x_3} = 0,\ \sigma_{13}^{(s)\pm} = 0,\ \sigma_{11}^{(s)\pm} = \psi^{(s)\pm}, \tag{16}$$

and on the end surfaces $x_1 = \pm d$ of the plate are written in the form

$$\frac{\partial \psi_*^{(s)\pm}}{\partial x_3} + \frac{\partial \sigma_{*13}^{(s)\pm}}{\partial x_1} = 0,\ \sigma_{*13}^{(s)\pm} = 0,\ \sigma_{*33}^{(s)\pm} = \psi_*^{(s)\pm}. \tag{17}$$

The symbol $*$ in (17) means that these values are considered at the end sections of the plate $x_1 = \pm d$.
In the relations (11)-(17), the dimensional Cartesian coordinates are used.

3. Methodology for constructing solutions to problems of electrodynamics, thermal conductivity and quasi-static thermoelasticity

To find the determining functions

$$\Phi = \{H_2(x_1,x_3,t); T(x_1,x_3,t); \sigma_{11}(x_1,x_3,t); \sigma_{13}(x_1,x_3,t); \sigma_{22}(x_1,x_3,t); \sigma_{33}(x_1,x_3,t)\}$$

their distribution over the thickness variable x_3 by cubic polynomials [19] are approximated:

$$\Phi(x_1,x_3,t) = \sum_{j=1}^{3} a_{(j-1)}^{\Phi}(x_1,t) x_3^{j-1}. \tag{18}$$

The coefficients $a_{(j-1)}^{\Phi}(x_1,t)$ of the approximation polynomials (18) are written in terms of the integral characteristics $\Phi_s(x_1,t)$ of the determining functions $\Phi(x_1,x_3,t)$

$$\Phi_s(x_1,t) = \frac{2s-1}{2} \int_{-1}^{1} \Phi(x_l,x_3,t) x_3^{s-1} dx_3\ \ (s = 1,\ 2) \tag{19}$$

and the boundary values $\Phi^{\pm}(x_1,t)$ of these functions on the surfaces $x_3 = \pm h$ are given. The equation for determining the integral characteristics $\Phi_s(x_1,t)$ is obtained by multiplying equations (1), (7), (11)-(13) by x_3^{s-1} and their integration over the variable x_3, taking into account the formulas (18), (19).

The resulting systems of initial equations for finding the integral characteristics $\Phi_s(x_1,t)$ $(s = 1,\ 2)$ of the determining functions will be systems of one-dimensional equations in the spatial variable x_1.

To find their solutions, we use finite integral transforms in the variable x_1 in accordance with the boundary conditions imposed on the determining functions at the end sections $x_1 = \pm d$ of the plate under consideration. Note that the integral characteristics H_{2s} of the component $H_2(x_1,x_3,t)$ of the magnetic field strength vector and the temperature T_s are also determined using the Laplace integral transform in the time variable t.

A detailed description of the method of determining the function $H_2(x_1,x_3,t)$ and the temperature T is presented in the paper [20]. Since the purpose of this work is to study the thermomechanical behavior of an electroconductive plate under the action of a quasi-static EMF, we will further use the methodology for constructing a solution to the two-dimensional quasi-static problem of thermoelasticity in stresses, presented in the work [19] and tested in the articles [14, 15].

The general procedure for obtaining a solution to the quasi-static thermoelasticity problem in terms of stresses is outlined below.

To solve the formulated quasi-static thermoelasticity problem for the plate, governed by (11)-(15), the distribution of the functions $\psi^{(s)}(x_1,x_3)$ and $\sigma_{13}^{(s)}(x_1,x_3)$ across the thickness coordinate x_3 are first approximated using cubic polynomial expressions:

$$\psi^{(s)} = \sum_{j=1}^{4} \psi_{j-1}^{(s)}(x_1) x_3^{j-1}. \tag{20}$$

$$\sigma_{13}^{(s)} = \sum_{j=1}^{4} \alpha_{13(j-1)}^{(s)}(x_1) x_3^{j-1}. \tag{21}$$

Then, the coefficients $\psi_{j-1}^{(s)}, \alpha_{13(j-1)}^{(s)}$ of the approximation polynomials (20), (21) are expressed in terms of integral characteristics

$$N^{(s)} = \frac{1}{2h}\int_{-h}^{h} \psi^{(s)} dx_3; \qquad M^{(s)} = \frac{3}{2h^2}\int_{-h}^{h} \psi^{(s)} x_3 dx_3;$$

$$N_{13}^{(s)} = \frac{1}{2h}\int_{-h}^{h} \sigma_{13}^{(s)} dx_3; \qquad M_{13}^{(s)} = \frac{3}{2h^2}\int_{-h}^{h} \sigma_{13}^{(s)} x_3 dx_3 \tag{22}$$

of the functions $\psi^{(s)}(x_1,x_3)$ and $\sigma_{13}^{(s)}(x_1,x_3)$ on the thickness coordinate x_3 and the boundary values of these functions as follows

$$\psi_{(0)}^{(s)} = \frac{3}{2}N^{(s)} - \frac{1}{4}\psi_{*}^{(s)}; \quad \psi_{(1)}^{(s)} = \frac{5}{2h}M^{(s)} - \frac{3}{4h}\psi_{**}^{(s)};$$

$$\psi_{(2)}^{(s)} = \frac{3}{4h^2}\psi_{*}^{(s)} - \frac{3}{2h^2}N^{(s)}; \quad \psi_{(3)}^{(s)} = \frac{5}{4h^3}\psi_{**}^{(s)} - \frac{5}{2h^2}M^{(s)};$$

$$\alpha_{13(0)}^{(s)} = \frac{3}{2}N_{13}^{(s)}; \quad \alpha_{13(1)}^{(s)} = \frac{5}{2h}M_{13}^{(s)};$$

$$\alpha_{13(2)}^{(s)} = -\frac{3}{2h^2}N_{13}^{(s)}; \quad \alpha_{13(3)}^{(s)} = -\frac{5}{2h^3}M_{13}^{(s)}. \tag{23}$$

Here,

$$\psi_{*}^{(s)} = \psi^{(s)+} + \psi^{(s)-}; \qquad \psi_{**}^{(s)} = \psi^{(s)+} - \psi^{(s)-}.$$

The system of equations for determining the integral characteristics $N^{(s)}$, $M^{(s)}$, $N_{13}^{(s)}$, and $M_{13}^{(s)}$ (analogs of forces and moments), is obtained by averaging the first two equations of the system (11)-(15) over the thickness coordinate x_3, and these equations multiplied by x_3, according to the formulas (22). As a result of the transformations performed, the integral characteristics $N^{(s)}$, $M^{(s)}$, $N_{13}^{(s)}$, $M_{13}^{(s)}$ are determined from the system of one-dimensional equations

$$\left(\frac{\partial^2}{\partial x_1^2} - \frac{3}{h^2}\right)N^{(s)} = \Phi_1^{(s)} - \frac{3}{2h^2}\psi_{*}^{(s)}, \tag{24}$$

$$\left(\frac{\partial^2}{\partial x_1^2} - \frac{15}{h^2}\right)M^{(s)} = \Phi_2^{(s)} - \frac{15}{2h^2}\psi_{**}^{(s)}, \tag{25}$$

$$\left(\frac{\partial^2}{\partial x_1^2} - \frac{3}{h^2}\right)N_{13}^{(s)} = \frac{1}{2h}\frac{\partial \psi_{**}^{(s)}}{\partial x_1}, \tag{26}$$

$$\left(\frac{\partial^2}{\partial x_1^2} - \frac{15}{h^2}\right)M_{13}^{(s)} = \frac{3}{2h}\frac{\partial \psi_{*}^{(s)}}{\partial x_1} - \frac{3}{h}\frac{\partial N^{(s)}}{\partial x_1}. \tag{27}$$

Here,

$$\Phi_1^{(s)} = -\frac{\alpha E}{1-\nu}\left\{\frac{\partial^2 T_1}{\partial x_1^2} + \frac{1}{2h}\left[\left(\frac{\partial T}{\partial x_3}\right)^{+} - \left(\frac{\partial T}{\partial x_3}\right)^{-}\right]\right\};$$

$$\Phi_2^{(s)} = -\frac{\alpha E}{1-\nu}\left\{\frac{\partial^2 T_2}{\partial x_1^2} + \frac{3}{2h}\left[\left(\frac{\partial T}{\partial x_3}\right)^{+} + \left(\frac{\partial T}{\partial x_3}\right)^{-}\right] - \frac{3}{2h^2}(T^{+} - T^{-})\right\},$$

where $T_n = \dfrac{2n-1}{2h^n}\displaystyle\int_{-h}^{h} T x_3^{n-1} dx_3$, $(n = 1,2)$ are integral temperature characteristics; $\left(\dfrac{\partial T}{\partial x_3}\right)^{\pm} = \dfrac{\partial T(x_1, \pm h, t)}{\partial x_3}$.

The boundary values of $\psi^{(s)\pm}$ of the function $\psi^{(s)}$ on the surfaces $x_3 = \pm h$, which are included in the system of equations (9)-(12) are found by averaging the boundary conditions (16), (17) in accordance with the relations (22).

In the case of a plate with end sections free from external force load $x_1 = \pm d$, the conditions for conjugation of the values of the functions $\psi(x_1, \tau)$ and $\sigma_{13}(x_1, \tau)$ (the component of the stress tensor) at the vertices of the rectangle of the plate cross-section are taken into account:

$$\begin{aligned} &\psi(d,\tau) = \psi(1,\tau); \quad \psi(d,\tau) = \psi(-1,\tau); \\ &\psi(-d,\tau) = \psi(1,\tau); \quad \psi(-d,\tau) = \psi(-1,\tau). \end{aligned}$$

$$\begin{aligned} &\sigma_{13}(d,\tau) = \sigma_{13}(1,\tau); \quad \sigma_{13}(d,\tau) = \sigma_{13}(-1,\tau); \\ &\sigma_{13}(-d,\tau) = \sigma_{13}(1,\tau); \quad \sigma_{13}(-d,\tau) = \sigma_{13}(-1,\tau). \end{aligned} \tag{28}$$

By averaging the boundary conditions at the end sections according to the formula (22), the corresponding boundary conditions along the x_1 coordinate on the functions $\psi^{\pm}$, N, M, N_{13}, M_{13} are obtained.

To solve the system of interdependent equations (24)-(27), a finite integral transform with respect to the variable x_1 is employed. The transform kernel is chosen as

$$K(\alpha_k, x_1) = \frac{\sin \alpha_k (x_1 + d)}{\sqrt{d}}, \quad \text{where} \quad \alpha_k = \frac{\pi k}{2d}.$$

Solutions to the formulated quasi-static thermoelasticity problem have been reported in [19], and these results were subsequently employed in [14] and [15].

Once the functions $\psi^{(s)}$ and $\sigma_{11}^{(s)}$ are known, the components $\sigma_{22}^{(s)}$, $\sigma_{33}^{(s)}$ of the stress tensor can be evaluated using relations (14) and (15).

To characterize the thermomechanical response of the considered plate, the stress intensity σ_i is introduced. For the present two-dimensional thermoelastic formulation, it is defined by [21]

$$\sigma_i = \frac{1}{2}\sqrt{(\sigma_{11} - \sigma_{22})^2 + (\sigma_{22} - \sigma_{33})^2 + (\sigma_{33} - \sigma_{11})^2 + 6\sigma_{13}^2}. \tag{29}$$

4. Analysis of the stress intensities of a lead plate under its induction heating by a homogeneous quasi-static EMF

Let us consider the induction heating of an electroconductive plate by a homogeneous quasi-static EMF. Accordingly, the values of the component $H_2(x_1,\ x_3,\ \tau)$ of the magnetic field intensity vector $\vec{H}$ at the bases $x_3 = \pm 1$ and end sections $x_1 = \pm d$ of the plate are given by the expressions:

$$H_2(x_1,\ \pm 1,\ \tau) = H_0 \varphi(\tau) e^{ib\tau}, \quad H_2(\pm d,\ x_3,\ \tau) = H_0 \varphi(\tau) e^{ib\tau}. \tag{30}$$

At the same time, the conditions (4) of matching the values of the functions $H_2^{\pm(0)}$ and $H_2^{\pm(0)*}$ and the condition (28) the conjugation of the values of the functions $\psi^{(s)}$ and $\sigma_{13}^{(s)}$ at the corner points of the plate cross section are fulfilled identically.

In the expressions (30), the function $\varphi(\tau)$ has the form:

$$\varphi(\tau) = 1 - e^{\beta\tau}. \tag{31}$$

Here $i = \sqrt{-1}$; $b = 1/\left(2\delta_0^2\right)$; $\delta_0 = \left(2\omega\sigma\mu h^2\right)^{-1/2}$ is a parameter that determines the depth of penetration of induction currents of frequency ω relative to the half--thickness of the plate h; $\beta = \ln\varepsilon/\tau_*$; τ_* is the dimensionless time corresponding to the output of electromagnetic oscillations of frequency ω to the steady state with amplitude H_0; $\varepsilon = 0.001$.

Substituting the expressions (30) into the corresponding formulas, taking into account (18), (19), the expression of the component $H_2(x_1,\, x_3,\, \tau)$ of the magnetic field strength vector $\vec{H}$ is obtained. Using the formula (6), the specific heat density of Joule Q is found. The resulting expression for Q is then incorporated into the corresponding relations presented in [20], which enables determination of the temperature field $T(x_1, x_3, Fo)$ within the plate.

According to the found expression of the temperature field $T(x_1, x_3, Fo)$ based on the relations (20)-(28), the expressions of the function $\psi(x_1, x_3, Fo)$ and the components $\sigma_{13}(x_1, x_3, Fo)$ and $\sigma_{11}(x_1, x_3, Fo)$ of the quasi-static stress tensor are obtained. According to these functions found from the relations (14)-(15), the expressions of the components $\sigma_{33}(x_1, x_3, Fo)$ and $\sigma_{22}(x_1, x_3, Fo)$ of the quasi-static stress tensor are found.

The numerical experiment was performed for an ideal lead plate using its physical and mechanical properties given in the Table 1 [22].

Table 1. Physical and mechanical properties of lead

Property	**Symbol**	**Value**
Electrical conductivity	σ	$0.48 \cdot 10^7$ Ωm^{-1}
Thermal conductivity	λ	35.3 W/(m · K)
Thermal diffusivity coefficient	κ	$0.25 \cdot 10^{-4}$ m^2/s
Poisson's ratio	ν	0.44
Young's modulus	E	$0.16 \cdot 10^5$ Pa
Coefficient of linear thermal expansion	α	$0.289 \cdot 10^{-4}$ K^{-1}

The thickness of the plate is $2h = 2$ mm, the width is $2d_* = 80$ mm (relative half-width of the plate is $d = 40$). The calculations were performed for two values of the parameter relative to the half-thickness of the plate h of the induction current penetration depth:

1) $\delta_0 = 0.1$ corresponds to near-surface heating;

2) $\delta_0 = 1$ corresponds to in-depth heating.

The circular frequency of electromagnetic oscillations $\omega_1 = 8.28 \cdot 10^6$ 1/s corresponds to the surface heating of the plate under consideration, and the circular

frequency of electromagnetic oscillations $\omega_2 = 8.28 \cdot 10^4$ 1/s corresponds to the in-depth heating.

Figure 2 shows the change in the dimensionless Fourier time Fo of the stress intensities σ_i/H_0^2 under near-surface $\delta_0 = 0.1$ induction heating with quasi-static EMF at the value of the Biot criterion $Bi = 0.1$ (a); $Bi = 1$ (b) at the characteristic points M_1 $(0.25\,d, 0.25)$, M_2 $(0.5\,d, 0.5)$, M_3 $(0.9\,d, 0.9)$ of a rectangle of cross-section of a lead plate.

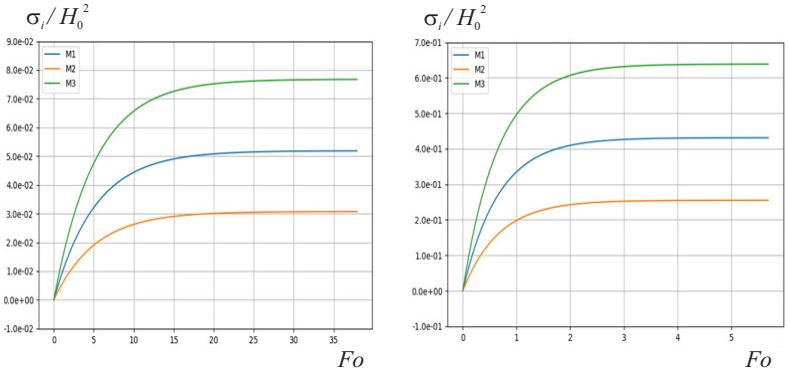

(a) (b)

Fig. 2. Time variation Fo of the stress intensities σ_i/H_0^2 under near-surface $\delta_0 = 0.1$ induction heating with quasi-static EMF at the value of the Biot criterion $Bi = 0.1$ (a); $Bi = 1$ (b) at the characteristic points M_1 $(0.25\,d, 0.25)$, M_2 $(0.5\,d, 0.5)$, M_3 $(0.9\,d, 0.9)$ of a rectangle of cross-section of a lead plate

Figure 3 shows the change in stress intensities σ_i/H_0^2 over the cross-sectional area of a plate under consideration and the Fourier time $Fo = 4$ (corresponding to the time when the stress intensity reaches its maximum value) under near-surface induction heating with quasi-static EMF at the value of the Biot criterion $Bi = 0.1$ (a); $Bi = 1$ (b).

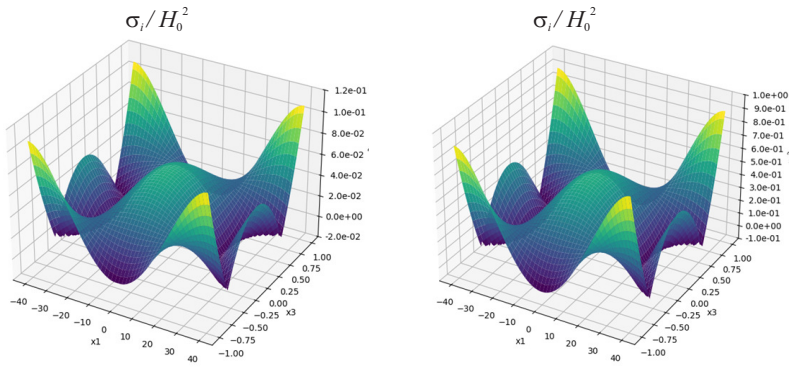

(a) (b)

Fig. 3. Variation of the stress intensities σ_i/H_0^2 over the cross-sectional area of a plate under near-surface $\delta_0 = 0.1$ induction heating with quasi-static EMF at the value of the Biot criterion $Bi = 0.1$ (a); $Bi = 1$ (b)

Figure 4 shows the change in the dimensionless Fourier time Fo of the stress intensities σ_i/H_0^2 under in-depth $\delta_0 = 1$ induction heating with quasi-static EMF at the value of the Biot criterion $Bi = 0.1$ (a); $Bi = 1$ (b) at the characteristic points M_1 $(0.25\,d, 0.25)$, M_2 $(0.5\,d, 0.5)$, M_3 $(0.9\,d, 0.9)$ of a rectangle of cross-section of a lead plate.

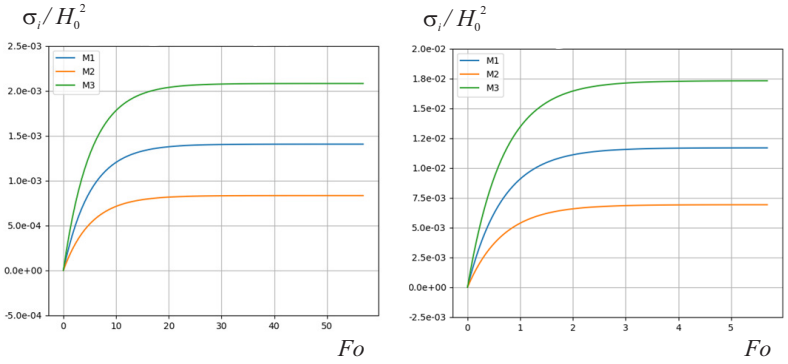

Fig. 4. Time variation Fo of the stress intensities σ_i/H_0^2 under in-depth $\delta_0 = 1$ induction heating with quasi-static EMF at the value of the Biot criterion $Bi = 0.1$ (a); $Bi = 1$ (b) at the characteristic points M_1 $(0.25\,d, 0.25)$, M_2 $(0.5\,d, 0.5)$, M_3 $(0.9\,d, 0.9)$ of a rectangle of cross-section of a lead plate

Figure 5 shows the change in stress intensities σ_i/H_0^2 over the cross-sectional area of a plate under consideration and the Fourier time $Fo = 4$ (corresponding to the time when the stress intensity reaches its maximum value) under in-depth $\delta_0 = 1$ induction heating with quasi-static EMF at the value of the Biot criterion $Bi = 0.1$ (a); $Bi = 1$ (b).

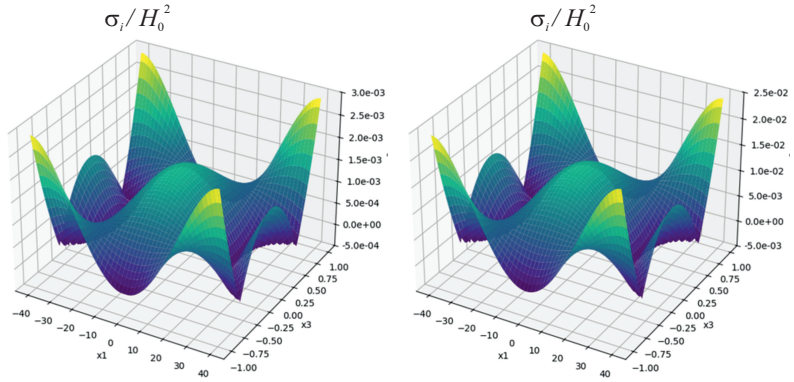

Fig. 5. Variation of the stress intensities σ_i/H_0^2 over the cross-sectional area of a plate under in-depth $\delta_0 = 1$ induction heating with quasi-static EMF at the value of the Biot criterion $Bi = 0.1$ (a); $Bi = 1$ (b)

Expressions of stress intensities σ_i/H_0^2 have the dimension $\mathrm{N}\cdot\mathrm{m}^2/\mathrm{A}^2$. Accordingly, the value of stress intensity is measured in Newtons N. As a result of the

numerical analysis of the change in time Fo of the stress intensities at the characteristic points M_1 $(0.25\,d,\,0.25)$, M_2 $(0.5\,d,\,0.5)$, M_3 $(0.9\,d,\,0.9)$ of a rectangle of cross-section of a lead plate of half-width $d = 40$ during its induction heating by a quasi-static EMF, it was found that: the maximum values of stress intensity in both cases – near-surface and in-depth heating – are obtained at the point M_3. This means that such values of stress intensity are achieved at the corner points of the cross--sectional rectangle, i.e., on the edges of the plate. In the case of near-surface heating at $\delta_0 = 0.1$, the maximum stress intensity values are approximately several times higher than their maximum values for in-depth heating at $\delta_0 = 1$.

5. Conclusions

In summary, this research reveals the following key findings:

1. The maximum values of stress tensor components and stress intensities in the considered plate during its induction heating with quasi-static EMF significantly depend on the dimensionless parameter δ_0 and the Biot criterion.
2. The time for stress intensities in the plate to reach steady state increases substantially with a one-order decrease in the Biot criterion.
3. Depending on the values of δ_0 and the Biot criterion, the distributions of stress intensities vary at selected characteristic points of the cross-section.
4. For a fixed δ_0 value, as the Biot criterion Bi value decreases, the values of stress intensities at characteristic points of the plate's cross-section become approximately equal. Specifically, when the value of the Biot criterion Bi equals 0.01, they nearly coincide due to the heating regime approaching conditions of thermal insulation of the plate's lateral faces.
5. The values of stress intensities significantly depend on the dimensionless parameter δ_0. Under near-surface heating conditions with $\delta_0 = 0.1$ and the Biot criterion $Bi = 1$, the maximum values of these quantities are much larger compared to the conditions of in-depth heating with $\delta_0 = 1$ and the Biot criterion $Bi = 1$.
6. With an increase in the magnitude of H_0, corresponding to the amplitude of steady electromagnetic oscillations, in both considered cases of near-surface and in-depth induction heating, the maximum values of stress tensor components and stress intensities increase according to a quadratic law.
7. Experiments have shown that the elastic deformation limit of a lead plate is reached at stress intensities σ_i of 4-12 MPa. Based on the numerical analysis conducted according to Figures 2 and 4, it was established that the lead plate under consideration loses its load-bearing capacity as a structural element in the case of near-surface heating ($\delta_0 = 0.1$) at a value of $H_0 \approx 3 \cdot 10^3$ A/m, and in the case of deep heating ($\delta_0 = 1$) at $H_0 \approx 3 \cdot 10^4$ A/m, respectively.

The numerical analysis of the thermostressed state of a lead plate performed in this paper and the new regularities of the behavior of the studied stress intensities

depending on the conditions of induction heating and convective heat transfer are of great theoretical and applied importance in the practice of engineering calculations for predicting the bearing capacity of electroconductive plate elements subjected to an external quasi-static electromagnetic field.

References

[1] Safari, A., Rafie, P., Taeb, Sh., Najafi, M., & Mortazavi, S.M.J. (2024). Development of lead--free materials for radiation shielding in medical settings: A review. *Journal of Biomedical Physics and Engineering*, *14*(3), 229-244. DOI: 10.31661/jbpe.v0i0.2404-1742.

[2] Wani, A.L., Ara, A., & Usmani, J.A. (2015). Lead toxicity: A review. *Interdisciplinary Toxicology*, *8*(2), 55-64. DOI: 10.1515/intox-2015-0009.

[3] Chang, Q., Guo, S., & Zhang, X. (2023). Radiation shielding polymer composites: Ray--interaction mechanism, structural design, manufacture and biomedical applications. *Materials & Design*, *233*, 112253. DOI: 10.1016/j.matdes.2023.112253.

[4] Wang, R., Li, H., & Sun, H. (2019). Bismuth: Environmental pollution and health effects. *Encyclopedia of Environmental Health*, 415-423. DOI: 10.1016/B978-0-12-409548-9.11870-6.

[5] Geetha, S., Satheesh Kumar, K.K., Rao, C.R., Vijayan, M., & Trivedi, D.C. (2009). EMI shielding: Methods and materials – A review. *Journal of Applied Polymer Science*, *112*(4), 2073-2086.

[6] Zachariah, S.M., Grohens, Y., Kalarikkal, N., & Thomas, S. (2022). Hybrid materials for electromagnetic shielding: A review. *Polymer Composites*, *43*(5), 2507-2544.

[7] Lee, K.S., Kim, S.W., & Eom, D.H. (2011). Temperature distribution and bending behaviour of thick metal plate by high frequency induction heating. *Materials Research Innovations*, *15*(sup1), S283-S287. DOI: 10.1179/143307511X12858957674076.

[8] Areitioaurtena, M., Segurajauregi, U., Akujarvi, V., et al. (2021). A semi-analytical coupled simulation approach for induction heating. *Advanced Modeling and Simulation in Engineering Sciences*, *8*, 14. DOI: 10.1186/s40323-021-00199-0.

[9] Bobart, G.F. (2020). Induction heating. AccessScience (accessed on 15 May 2023). https:// www.accessscience.com/content/article/a341500.

[10] Musii, R., Pukach, P., Kohut, I., Vovk, M., & Slahor, L. (2022). Determination and analysis of Joule's heat and temperature in an electrically conductive plate element subject to short-term induction heating by a non-stationary electromagnetic field. *Energies*, *15*, 5250. DOI: 10.3390/ en15145250.

[11] Musii, R., Pukach, P., Melnyk, N., Vovk, M., & Slahor, L.U. (2023). Modeling of the temperature regimes in a layered bimetallic plate under short-term induction heating. *Energies*, *16*(13), 4980. DOI: 10.3390/en16134980.

[12] Cho, H., Park, J.S., Han, Y.S., Xu, G., & Sohn, D. (2024). Electromagnetic-thermal-mechanical coupling analysis of bent rotor straightening via electromagnetic induction heating. *Journal of Computational Design and Engineering*, *11*(6), 283-299.

[13] Xue, F., He, D., Zhou, H., Zhou, H., & Sun, Y. (2024). Optimization research on inductor structural parameters for post-weld electromagnetic induction heating pulsation aging treatment of large aluminum components. *Case Studies in Thermal Engineering*, *63*, 105372.

[14] Musii, R., Klapchuk, M., Koda, E., Kernytskyy, I., Svidrak, I., Humeniuk, R., ... & Royko, Y. (2025). Analysis based on a two-dimensional mathematical model of the thermo-stressed state of a copper plate during its induction heat treatment. *Symmetry*, *17*(5), 754.

[15] Musii, R., Pabyrivskyi, V., Klapchuk, M., Całus, D., Gębara, P., Kohut, Z., & Szymczykiewicz, E. (2025). Mathematical modeling and analysis of the mechanical properties of a nonferromagnetic panel under the action of a quasi-steady electromagnetic field. *Energies*, *18*(14), 3680. DOI: 10.3390/en18143680.

[16] Ida, N. (2015). *Engineering Electromagnetics*. Springer International Publishing Switzerland.

[17] Holman, J.P. (2009). *Heat Transfer*. McGraw-Hill.

[18] Rudnev, V., Loveless, D., & Cook, R.L. (2017). *Handbook of Induction Heating*. Second Edition. CRC Press. DOI: 10.1201/9781315117485.

[19] Musii, R.S. (2024). Constructing solutions for two-dimensional quasi-static problems of thermomechanics in terms of stresses for bodies with plane-parallel boundaries. *Mathematical Modeling and Computing*, *11*(4), 995-1002. DOI: 10.23939/mmc2024.04.995.

[20] Musii, R., Lis, M., Pukach, P., Chaban, A., Szafraniec, A., Vovk, M., & Melnyk, N. (2024). Analysis of varying temperature regimes in a conductive plate during induction heating under a quasi-steady electromagnetic field. *Energies*, *17*(2), 366. DOI: 10.3390/en17020366.

[21] Goodier, J.N., & Hodge Jr, P.G. (2016). *Elasticity and Plasticity: The Mathematical Theory of Elasticity and the Mathematical Theory of Plasticity*. Courier Dover Publications.

[22] Thompson, M. (2006). *Base Metals Handbook*. Woodhead Publishing. DOI: 10.1016/B978-1-84569-154-7.50009-8.